Earth and Planetary Science Letters 310 (2011) 252–261

Contents lists available at SciVerse ScienceDirect

Earth and Planetary Science Letters

journal homepage: www.elsevier.com/locate/epsl

Plate tectonics on super-Earths: Equally or more likely than on Earth

H.J. van Heck *, P.J. Tackley

Department of Earth Sciences, ETH Zürich, Sonneggstrasse 5, 8092 Zürich, Switzerland

ARTICLE INFO

Article history:
Received 17 December 2010
Received in revised form 29 May 2011
Accepted 29 July 2011
Available online xxxx

Editor: Y. Ricard

Keywords:
super-Earths
plate tectonics
mantle convection

ABSTRACT

The discovery of extra-solar super-Earths has prompted interest in their possible mantle dynamics and evolution, and in whether their lithospheres are most likely to be undergoing active plate tectonics like on Earth, or be stagnant lids like on Mars and Venus. The origin of plate tectonics is poorly understood for Earth, likely involving a complex interplay of rheological, compositional, melting and thermal effects, which makes it challenging to make reliable predictions for other planets. Nevertheless, as a starting point it is common to parameterize the complex processes involved as a simple yield stress that is either constant or has a Byerlee's law dependence on pressure. Because the simplifying assumptions made in developing analytical scalings may not be valid over all parameter ranges, numerical simulations are needed; one numerical study on super-Earths finds that plate tectonics is less likely on a larger planet (O'Neill and Lenardic (2007)), in apparent contradiction of an analytical scaling study (Valencia et al. (2007)). To try and understand this we here present new calculations of yielding-induced plate tectonics as a function of planet size, focusing on the idealized end members of internal heating or basal heating as well as different strength profiles, and compared to analytical scalings. In the present study we model super-Earths as simple scaled up versions of Earth, i.e., assuming constant physical properties, keeping the ratio of core/mantle radii constant and applying the same temperature difference between top/bottom boundaries and the same internal heating rate. Effects that originate outside of the planet, such as tidal forces, meteor impacts and intense surface heating from a nearby star are not considered. We find that for internally-heated convection plate tectonics is equally likely for terrestrial planets of any size, whereas for basally-heated convection plate tectonics becomes more likely with increasing planet size. This is indicated both by analytical scalings and the presented numerical results, which agree with each other. When scalings are adjusted to account for increasing mean density with increasing planet size, plate tectonics becomes more likely with increasing planet size for all scenarios. The influence of the pressure variation of viscosity, thermal expansivity and conductivity may, however, act in the opposite sense and needs to be determined in future studies. At least in the simplest case, factors other than planet size, such as the presence of surface water, are likely most important for determining the presence or absence of plate tectonics.

1. Introduction

Table 1
Fig. 5

Super-Earths are terrestrial planets outside our solar system with masses up to about ten times the mass of Earth. Any planet with more mass than this is unlikely to be terrestrial (Ida and Lin, 2004). Observations of super-Earths are indirect and the best constrained properties of such planets are basic properties like their masses and distance to their star. In recent years many super-Earths have been found, and many more are expected to be found in the near future, in particular by the NASA Kepler mission (kepler.nasa.gov), which is searching the skies for planets that are the same size as Earth. So far, over 700 targets with viable exoplanet candidates with sizes as small as that of Earth to larger than that of Jupiter have been found. Arguably the most fundamental question one can ask about super-Earths is: "Do we expect super-Earths to have active plate tectonics, like the Earth, or do we expect them to be in the stagnant lid mode, like present day Mars and Venus?" Since both data about super-Earths is scarce, and the complex processes of plate tectonics and subduction initiation are not very well understood it is unlikely that, at the moment, a robust prediction can be made about the convective regime of one particular exoplanet. We can however build a general theory about terrestrial planets of all sizes. Previous efforts in this direction were made by Valencia et al. (2007), O'Neill and Lenardic (2007), Tackley and van Heck (2008), Valencia and O'Connell (2009) and Korenaga (2010a) and Korenaga (2010b). Valencia et al. (2007) used a parameterized convection model, based on scaling laws, to conclude that the likelihood of plate tectonics increases with planet size. Their model predicts a decrease in plate thickness

* Corresponding author.
E-mail addresses: hvanheck@erdw.ethz.ch, grotebaas@hotmail.com (H.J. van Heck).

0012-821X/$ – see front matter © 2011 Elsevier B.V. All rights reserved.
doi:10.1016/j.epsl.2011.07.029

Table 1
Parameters that scale with planet size. The stress factor and friction coefficient factor are used to translate non-dimensional stresses to dimensional stresses and friction coefficient. The values listed in Table 2 are used to calculate them.

Size (S)	Rayleigh (Ra)	Heating rate ($\tilde{H}$)	Stress factor ($\frac{D^2}{\kappa\eta_0}$)	Fric. c. factor ($\frac{D^3}{\kappa\eta_0\rho g}$)
1	$5.0*10^7$	10	$8.352*10^{-3}$	0.731
1.25	$12.2*10^7$	15.6	$13.05*10^{-3}$	1.143
1.5	$25.3*10^7$	22.5	$18.79*10^{-3}$	1.645
1.75	$46.9*10^7$	30.6	$25.58*10^{-3}$	2.239
2	$80.0*10^7$	40	$33.41*10^{-3}$	2.924

and an increase of shear stresses with increasing planet size, leading them to conclude that plate tectonics is inevitable on super-Earths. O'Neill and Lenardic (2007) reached opposite conclusions, stating that stagnant lid convection is the more likely convective regime on super-Earths. The approach they used is similar to ours, using a numerical model to simulate convection on Earth and scale that to bigger planets. O'Neill and Lenardic (2007) found that the dominant effect was the more rapid increase in pressure with depth on more massive planets. This effect leads to an increase in fault strength hence a stronger lithosphere and thus a lower likelihood of plate tectonics. Korenaga (2010a) shows that, (based on empirical analytical scaling relationships for temperature dependent convection with a visco-plastic rheology, Korenaga, 2010b) plate tectonics becomes more likely with increasing planet size.

As oceanic plates act as the upper thermal boundary layer of mantle convection, and continents are formed from the mantle, it is desirable to treat mantle and plates as a single, integrated system rather than two separate entities. Although in recent years progress has been made in both the comprehensiveness and clarity of numerical models, (see Bercovici, 2003 for a review) basic questions about why the Earth is currently the only terrestrial planet with active plate tectonics, which parameters control the formation of plates, and which processes are responsible for the creation of subduction zones and spreading centers, remain without definitive answers, although several hypotheses exist.

Convection with temperature dependent viscosity displays three different regimes, none of which is plate-like. Solomatov (1995) and Moresi and Solomatov (1995) conducted numerical experiments of convection with large viscosity contrasts. They found distinct different regimes in which the cold upper boundary layer did or did not participate in convection, separating a stagnant lid regime from a mobile and a sluggish lid regime. Models got much closer to including plate-like behavior when Moresi and Solomatov (1998) introduced a yield stress. When the stress reaches a certain critical stress, the lithospere is weakened by yielding, allowing spreading centers and subduction-like features to form. This approach was used in 3D

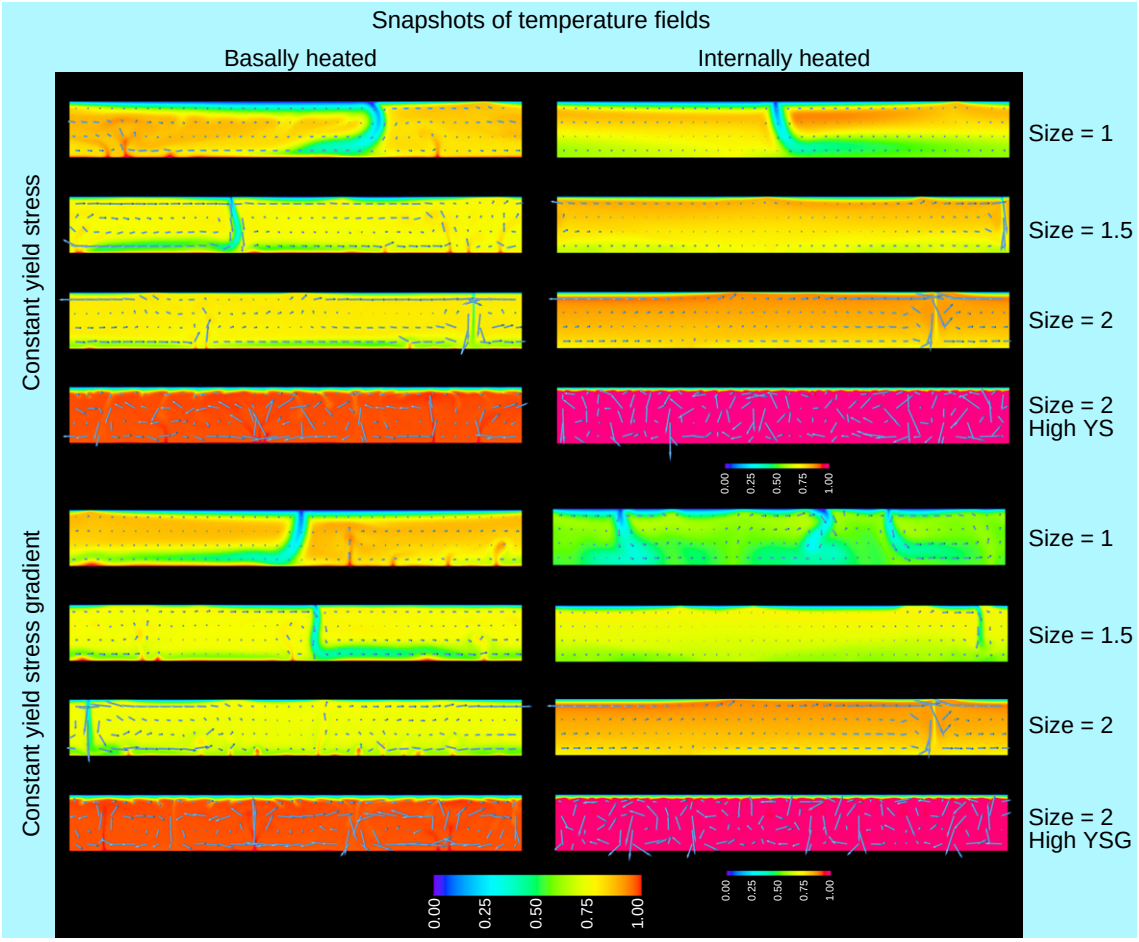

Fig. 1. Snapshots of the temperature field with arrows indicating the velocity field for representative cases. In the left column images of cases that are basally-heated, in the right column cases that are internally-heated. The top four rows have a constant yield stress, the bottom four rows a constant yield stress gradient. For each scenario four snapshots are shown: mobile lid convection for size 1, 1.5 and 2, plus stagnant lid convection (with a higher yield stress or yield stress gradient) for size 2. For the images showing a stagnant lid regime a different color scale is used as indicated since (non-dimensional) internal temperatures exceed 1. (For interpretation of the references to color in this figure legend, the reader is referred to the web version of this article.)

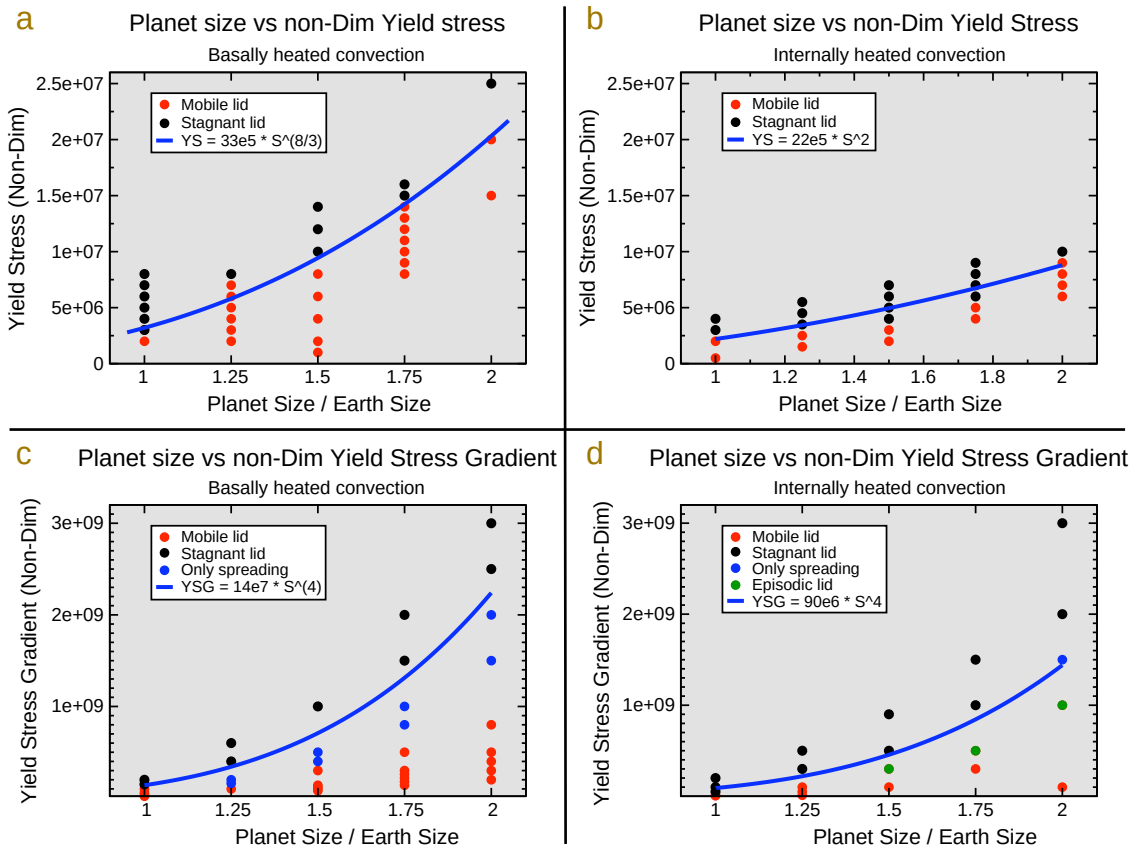

Fig. 2. Overview of the results of the calculations. Nondimensional yield stress or yield stress gradient versus planet size for the four different end-member scenarios. a. Basally heated convection and constant yield stress; b. Internally heated convection and yield stress gradient; c. Basally heated convection and constant yield stress; d. Internally heated convection and yield stress gradient. The analytical predictions between planet size and yield stress (−gradient) are indicated by the blue lines, multiplied by a coefficient to fit the numerical results. (For interpretation of the references to color in this figure legend, the reader is referred to the web version of this article.)

Cartesian geometry by Trompert and Hansen (1998) and Tackley (2000a). In general, these studies found three distinctive convective regimes: mobile lid, where the lithosphere is constantly yielding, allowing zones of subduction and spreading centers to be present at all times, a stagnant lid, where one continuous plate covers the whole domain, and episodic lid, where the regime keeps changing from mobile lid to stagnant lid, back to mobile lid over time. Later some studies included more Earth-like features such as history dependent weakening (Tackley, 2000b, Ogawa, 2003) and a low viscosity asthenosphere (Tackley, 2000b, Richards et al., 2001). Stein et al. (2004) used a similar but more extensive approach to study, among others, the influence of temperature, stress and pressure dependence of the viscosity on plate-like behavior. Solomatov (2004) discussed how subduction can be initiated by small scale convection. Muhlhaus and Regenauer-Lieb (2005) discussed the importance of elasticity and non-Newtonian rheology. More recently, Loddoch et al. (2006) argued that a fourth regime exists between the stagnant and episodic lid, where different scalings apply. van Heck and Tackley (2008) and Foley and Becker (2009) applied these techniques to study the behavior of self consistent plate tectonics in fully 3D-spherical geometry, and Yoshida (2008) used a similar model to study the wavelength of convection, and later continental breakup (Yoshida, 2010). This type of model has also been applied to other terrestrial planets; for example, Fowler and O'Brien (2003) used a model similar to the ones mentioned above to investigate the frequency of resurfacing events on Venus.

In the present study we derive analytical scalings, accompanied by results of numerical calculations, for a basic upscaling of the Earth to obtain first order predictions about the likelihood of plate tectonics on super-Earths. In upscaling planet size, care needs to be taken to scale all parameters that change with planet size consistently throughout the equations, particularly if using nondimensional units, as we do here. Some scalings are not immediately obvious, because they appear in the scaling factors used to convert nondimensional parameter values to their dimensional equivalents. The numerical model we use solves for the equations of thermal convection where plate tectonics and large scale mantle convection are treated as a single self consistent system, similar to van Heck and Tackley (2008).

2. Model description

The physical model we choose here to use to study the likelihood of plate tectonics on terrestrial planets is a general one to model fluid flow under the Boussinesq approximation, i.e. all material properties are assumed to be constant in both space and time except viscosity, which depends on temperature and stress through plastic yielding. This is a gross simplification of material properties on Earth, which also depend on pressure, but is in the spirit of the only other numerical studies on super-Earths to date (O'Neill and Lenardic, 2007, Korenaga, 2010a), furthermore it is important to establish scalings for a simple system before progressing to one with greater complexity. We do, however, derive the influence on scalings of pressure-dependent density, and qualitatively consider what effect other pressure-dependent properties might have. We use two different approaches to the same physical model: one analytical, based on scaling laws and boundary layer theory, and one numerical where we solve the coupled momentum, energy and continuity equations.

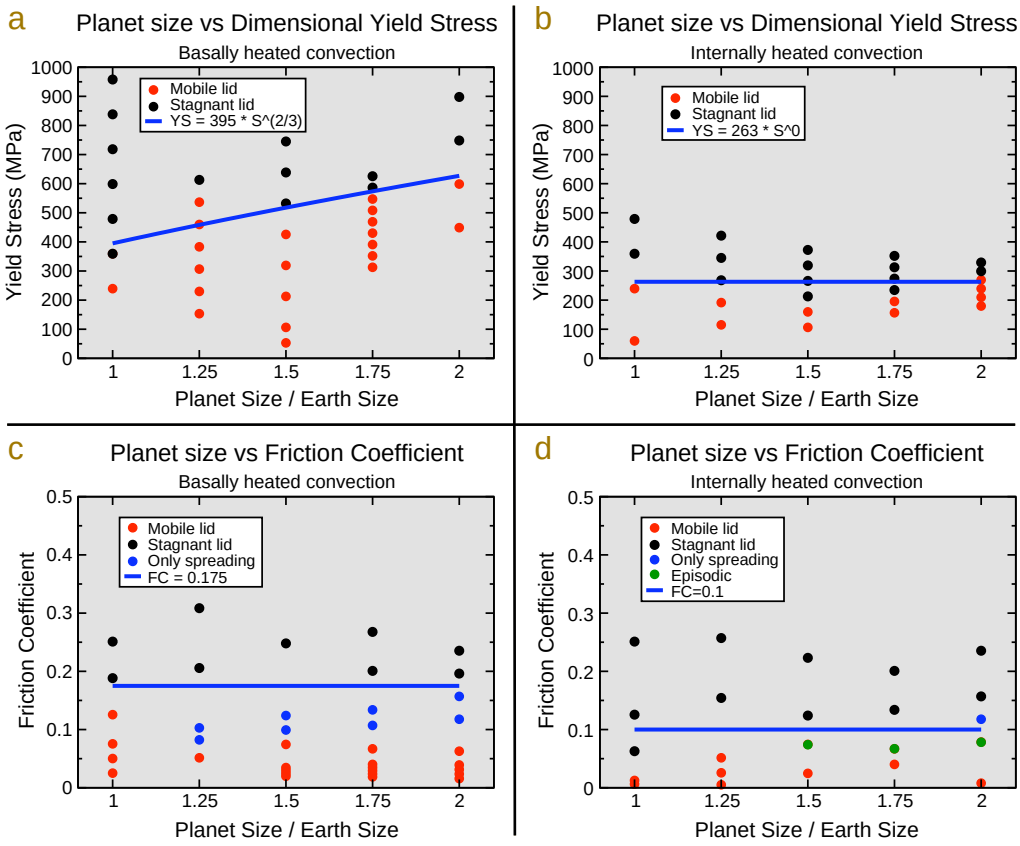

Fig. 3. Overview of the results of the calculations. Dimensional yield stress or friction coefficient versus planet size for the four different end-member scenarios. a. Basally heated convection and constant yield stress; b. Internally heated convection and yield stress gradient; c. Basally heated convection and constant yield stress; d. Internally heated convection and yield stress gradient. The analytical predictions between planet size and yield stress (or friction coefficient) are indicated by the blue lines, multiplied by a coefficient to fit the numerical results. (For interpretation of the references to color in this figure legend, the reader is referred to the web version of this article.)

The yield stress is assumed to either increase in proportion to depth, simulating increasing fault strength with pressure (i.e., Byerlee's law), or is kept constant, mimicking the semi-ductile, semi-brittle regime around the brittle-ductile transition (Kohlstedt et al., 1995). We focus on the end-member cases of purely internally-heated and purely basally-heated convection, and find predictions about the transition in convective regime (mobile versus stagnant lid) as a function of planet size.

The conservation equations are, in nondimensional form;

$$\nabla \cdot \underline{v} = 0, \tag{1}$$

$$\nabla \cdot \sigma_{ij} - \nabla p = RaT\,\underline{\hat{z}}, \tag{2}$$

$$\frac{\partial T}{\partial t} = \nabla^2 T - \underline{v} \cdot \nabla T + H, \tag{3}$$

where $\underline{v}$ is velocity, σ_{ij} is the deviatoric stress tensor ($=\eta(v_{i,j}+v_{j,i})$ where η is viscosity which in our model depends on temperature and stress), p the pressure, T the temperature, $\underline{\hat{z}}$ the vertical unit vector, t the time, and H the internal heating rate.

3. Analytical scalings

Here, S is the ratio of the planet's radius to Earth's radius. Four non-dimensional parameters need to be scaled with planet size (S): Rayleigh number (Ra), internal heating rate (H), yield stress (σ_y) and yield stress gradient ($d\sigma_y/dz$).

The Rayleigh number can be expressed as:

$$Ra = \frac{\rho g \alpha \triangle T D^3}{\eta_0 \kappa}, \tag{4}$$

where ρ, g, α, $\triangle T$, D, κ and η_0 are density, gravitational acceleration, temperature scale, depth of the mantle, thermal diffusivity and reference viscosity respectively.

In our model, the only two parameters in the Ra that change with S are g and D. Under the assumptions of constant core-mantle radius and incompressibility both scale proportional to S.

$$D \propto S, \tag{5}$$

$$g \propto \frac{M}{S^2} \propto \frac{S^3}{S^2} \propto S, \tag{6}$$

where M is the mass of the planet. Substituting into Eq. (4) leads to:

$$Ra \propto S^4. \tag{7}$$

The nondimensional internal heating rate is nondimensionalised via D^2 and thus scales as S^2. The stresses are non-dimensionalized via D^2, leading to scalings of the yield stress and the yield stress gradient of:

$$\tilde{H} = H\frac{D^2}{\kappa C_p \triangle T} \propto S^2, \tag{8}$$

$$\tilde{\sigma}_{\text{yield}} = \sigma_y \frac{D^2}{\kappa \eta_0} \propto S^2, \tag{9}$$

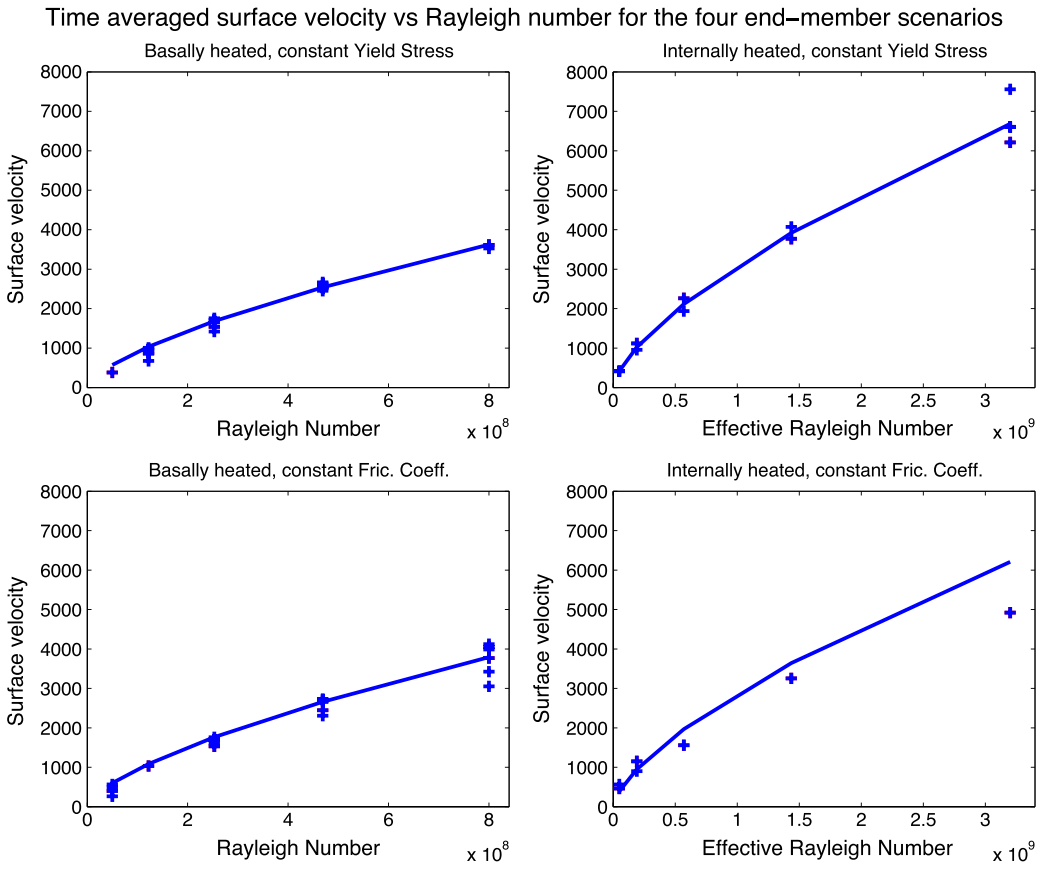

Fig. 4. The non-dimensional surface velocity was averaged over the second half of each calculation. The blue crosses indicate the calculations for stable mobile cases. The blue lines indicate the analytical prediction of; $vel. = c\,Ra^{\frac{2}{3}}$. The coefficient c was set to 1 for the basally heated cases and to 1.5 for the internally heated cases. The (effective) Rayleigh number can be translated to planet size (S) via Eq. (7) or (20) for basally and internally heated cases respectively. (For interpretation of the references to color in this figure legend, the reader is referred to the web version of this article.)

$$\frac{d\sigma_y}{dz} = c\rho g \propto S, \tag{10}$$

$$\frac{d\tilde{\sigma}_y}{d\tilde{z}} = \frac{d\sigma_y}{dz}\frac{D^2}{\kappa\eta_0} D \propto S^4, \tag{11}$$

where C_p, σ_y and c represent heat capacity, yield stress and friction coefficient respectively. Tildes are used to indicate non-dimensional quantities.

In order to predict the transition from mobile to stagnant lid convection we follow the reasoning of Moresi and Solomatov (1998). When the predicted convective stresses exceed the yield stress, yielding will take place and the mobile lid regime will be entered or sustained. When the yield stress exceeds the convective stresses a stagnant lid will form. Thus, we investigate how the ratio of (non-dimensional) convective stress/yield stress scales with S. The scaling of yield stress and yield stress gradient are described by Eqs. (9) and (11). To find the scaling of convective stresses we have to distinguish between internally and basally heated convection.

3.1. Analytical scalings: basally-heated convection

Three assumptions are made: The convective regime is a mobile lid mode, the interior viscosity remains approximately constant, and standard boundary layer theory can be applied to describe scalings between stress, velocity, Ra and Nusselt number (Nu) (Turcotte and Schubert, 1982). Under these assumptions the nondimensional convective stresses that act on the lithosphere will scale with planet size S as;

$$\tilde{\sigma}_{\text{convective}} \propto \eta_i \tilde{v} \propto v \propto Ra^{2/3} \propto S^{8/3}, \tag{12}$$

where η_i is the interior viscosity and v the velocity. Combining Eqs. (9) and (12) gives the result;

$$\frac{\tilde{\sigma}_{\text{convective}}}{\tilde{\sigma}_{\text{yield}}} \propto S^{2/3}, \tag{13}$$

which shows that that for constant (dimensional) yield stress, the nondimensional convective stresses increase more rapidly with planet size S than the nondimensional yield stress does. This makes the mobile regime more likely for large planets than for small ones.

For the depth-dependent yield stress, the appropriate yield stress to take is that at the base of the lithosphere, which is given by the thickness of the thermal boundary layer δ. Under the assumptions made, this thickness will scale with planet size $\tilde{S}$ as:

$$\tilde{\delta} \propto Nu^{-1} \propto Ra^{-1/3} \propto \tilde{S}^{-4/3}. \tag{14}$$

The effective yield stress (yield stress at the base of the lithosphere) for basally heated convection will scale as:

$$\tilde{\sigma}_{\text{yield-effective}} = \tilde{\delta}\frac{d\tilde{\sigma}}{d\tilde{z}} \propto \tilde{S}^{-4/3}\tilde{S}^4 \propto \tilde{S}^{8/3}, \tag{15}$$

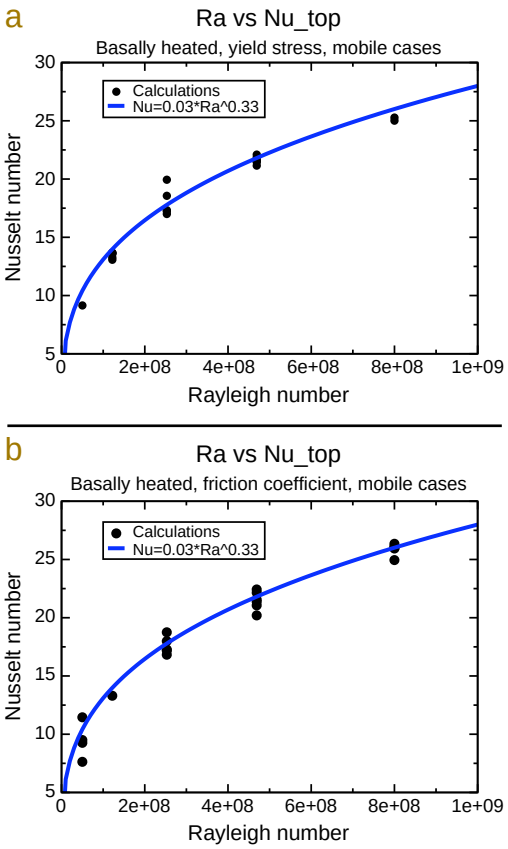

Fig. 5. Diagrams of Rayleigh number (Ra_0) versus surface Nusselt number for the two scenarios of basally heated convection. a. Basally heated convection and constant yield stress; b. Basally heated convection and constant yield stress gradient. Blackdots indicate results from the calculations (all mobile cases), the blue line represents the theoretical relationship. The numerical results agree well with the analytical scalings. (For interpretation of the references to color in this figure legend, the reader is referred to the web version of this article.)

Combining Eqs. (15) and (12) gives the result:

$$\frac{\tilde{\sigma}_{\text{convective}}}{\tilde{\sigma}_{\text{yield}-\text{effective}}} \propto S^0, \tag{16}$$

which shows that for basally heated convection and a depth dependent yield stress (i.e. friction coefficient) the transition from mobile to stagnant lid regime is independent of planet size S.

3.2. Analytical scalings: internally-heated convection

For internally-heated convection slightly different assumptions must be made. The surface heat flux is determined by the internal heating rate. The internal viscosity adjusts, through temperature changes, such that the given heat can be lost. The resulting change in internal temperature is small compared to global temperature variations. (i.e. the total temperature difference over the entire mantle can be assumed constant.) Given these assumptions we can derive how the convective stresses will scale with planet size S, for which we first need an expression for the Ra based on internal viscosity as function of S. Here, for continuity with the basally-heated scalings and because the internal temperature does not change much due to strong feedback between viscosity and temperature, the temperature-based Rayleigh number is still used rather than a heating-based Rayleigh number. The end result would be the same if the analysis were performed using a heating-based Rayleigh number.

$$Nu \propto H \propto S^2, \tag{17}$$

$$\left(Ra_{i0}\frac{S^4}{\eta_i/\eta_{i-\text{Earth}}}\right)^{1/3} \propto S^2, \tag{18}$$

$$\eta_i/\eta_{i-\text{Earth}} \propto S^{-2}, \tag{19}$$

$$Ra_i = Ra_{i0}\frac{S^4}{\eta_i/\eta_{i-\text{Earth}}} \propto S^6, \tag{20}$$

where η_i is the internal viscosity, $\eta_{i-\text{Earth}}$ is the internal viscosity for a planet of size 1, Ra_i is the Rayleigh number based on internal viscosity and Ra_{i0} is the Rayleigh number for a planet of size 1. With this new scaling for internal viscosity (19) and Ra_i (Eq. (20)) we can derive how the convective stresses scale with S.

$$\tilde{\sigma}_{\text{convective}} \propto (\eta_i/\eta_{i-\text{Earth}})\tilde{v} \propto S^{-2} Ra_i^{2/3} \propto S^2, \tag{21}$$

combining Eqs. (21) and (9) gives:

$$\frac{\tilde{\sigma}_{\text{convective}}}{\tilde{\sigma}_{\text{yield}}} \propto S^0. \tag{22}$$

For the depth dependent yield stress we can write that the effective yield stress scales as:

$$\tilde{\sigma}_{\text{yield}-\text{effective}} = \tilde{\delta}\frac{d\tilde{\sigma}_y}{d\tilde{z}} \propto S^{-2} S^4 \propto S^2, \tag{23}$$

combining 21 and 23:

$$\frac{\tilde{\sigma}_{\text{convective}}}{\tilde{\sigma}_{\text{yield}-\text{effective}}} \propto S^0. \tag{24}$$

Eqs. (22) and (24) show that for internally heated convection the transition from mobile to stagnant lid is expected to happen at the same (dimensional) yield stress or friction coefficient for each value of S, both for the constant and depth dependent yield stresses.

3.3. Influence of increasing density with planet size

Most physical parameters, including density, viscosity, thermal expansivity and thermal conductivity, depend on pressure, so their mean values will change with planet size. Here, for comparison with Valencia et al. (2007) and Valencia and O'Connell (2009), we consider the effect on the scalings of an increase in mean density with planet size. The mean density affects the scalings because it increases gravitational acceleration, total internal heating, and Rayleigh number. Here we consider how the above-derived scalings change due to this effect. Based on mean density (ρ_{mean}), Valencia et al. (2007) find that $S \propto M^{\frac{1}{4}}$, whereas in our above scalings with constant density $S \propto M^{\frac{1}{3}}$ was assumed. In this case, the mean density will change with planet size as;

$$\rho_{\text{mean}} \propto \frac{M}{S^3} \propto \frac{S^4}{S^3} \propto S, \tag{25}$$

while acceleration due to gravity now scales as;

$$g \propto \frac{M}{S^2} \propto \frac{S^4}{S^2} \propto S^2. \tag{26}$$

This will change the scaling of both Ra and yield stress gradient with planet size as follows;

$$Ra = \frac{\rho_{mean} g \alpha \triangle T D^3}{\eta_0 \kappa} \propto S S^2 S^3 \propto S^6, \tag{27}$$

$$\frac{d\sigma_y}{dz} = c\rho_{surface} g \propto S^2, \tag{28}$$

$$\frac{d\tilde{\sigma}}{d\tilde{z}} = \frac{d\sigma_y}{dz}\frac{D^2}{\kappa\eta_0} D \propto S^2 S^3 \propto S^5, \tag{29}$$

where $\rho_{surface}$ is the surface density, independent of planet size. Note that in this scenario Eqs. (26) and (27) replace Eqs (6) and (7), and Eqs. (28) and (29) replace Eqs (10) and (11).

Since the internal heating rate H is constant per unit mass, the nondimensional heating rate (Eq. (8)) does not change due to a change in density, even though the dimensional internal heating rate increases. The scaling of surface boundary layer thickness δ depends on the assumption made. If thermal conductivity (k) and heat capacity (C_p) are assumed to be constant (in which case thermal diffusivity (κ) will change with density) then the usual relation given in Eq. (30) applies. If instead, thermal diffusivity (κ) and heat capacity (C_p) are assumed constant then thermal conductivity ($k = \rho C_p \kappa$) will be lower at the surface than its average, so the surface boundary layer will have to be thinner in order to lose the same amount of heat. In this case the thermal boundary layer will scale as given by Eq. (31). This case is physically more realistic because then the surface value of k is the same for all planet sizes, and therefore we use it in subsequent analyses.

$$\tilde{\delta} \propto Ra^{-\frac{1}{3}}, \tag{30}$$

$$\tilde{\delta} \propto \frac{\rho_{surface}}{\rho_{mean}} Ra^{-\frac{1}{3}} \propto S^{-1} Ra^{-\frac{1}{3}}. \tag{31}$$

With these new relationships we can build analytical predictions for the four scenarios discussed above (internally heated versus basally heated and constant yield stress versus constant yield stress gradient) in the same way as before, by comparing the effect of planet size (S) on yield stress (gradient) to the effect on convective stress.

For basally heated convection combined with a constant yield stress, Eqs. (12) and (13) now become;

$$\tilde{\sigma}_{convective} \propto Ra^{\frac{2}{3}} \propto S^{\frac{12}{3}} = S^4, \tag{32}$$

$$\frac{\tilde{\sigma}_{convective}}{\tilde{\sigma}_{yield}} = \frac{S^4}{S^2} = S^2. \tag{33}$$

For basally heated convection combined with a constant yield stress gradient, and assuming constant κ (using Eq. (31)) gives;

$$\tilde{\sigma}_{yield-effective} = \delta \frac{d\tilde{\sigma}_y}{d\tilde{z}} \propto S^{-3} S^5 = S^2, \tag{34}$$

$$\frac{\tilde{\sigma}_{convective}}{\tilde{\sigma}_{yield-effective}} \propto \frac{S^4}{S^2} = S^2. \tag{35}$$

For internally-heated convection combined with a constant yield stress (with increasing density) Eqs. (17) to (22) have to be rewritten, since now, $Ra \propto S^6$ (Eq. (27)) in stead of $Ra o S^4$ (Eq. (7)).

$$Nu \propto H \propto S^2, \tag{36}$$

$$\left(Ra_{i0} \frac{S^6}{\eta_i / \eta_{i-Earth}}\right)^{1/3} \propto S^2, \tag{37}$$

$$\eta_i / \eta_{i-Earth} \propto S^0, \tag{38}$$

$$Ra_i = Ra_{i0} \frac{S^6}{\eta_i / \eta_{i-Earth}} \propto S^6, \tag{39}$$

$$\tilde{\sigma}_{convective} \propto (\eta_i / \eta_{i-Earth}) \tilde{v} \propto S^0 Ra_i^{2/3} \propto S^4. \tag{40}$$

Combining Eqs. (40) and (9) gives:

$$\frac{\tilde{\sigma}_{convective}}{\tilde{\sigma}_{yield}} \propto \frac{S^4}{S^2} \propto S^2. \tag{41}$$

For internally-heated convection combined with a constant yield stress gradient we again assume constant κ in determining the thickness of the lithosphere (δ). Assuming constant κ (using Eq. (31)) gives;

$$\tilde{\sigma}_{yield-effective} = \tilde{\delta} \frac{d\tilde{\sigma}_y}{d\tilde{z}} \propto S^{-3} S^5 = S^2, \tag{42}$$

$$\frac{\tilde{\sigma}_{convective}}{\tilde{\sigma}_{yield-effective}} \propto \frac{S^4}{S^2} = S^2. \tag{43}$$

Combined, the Eqs. (33), (35), (41) and (43) show that for all four scenarios investigated (basal versus internal heating mode and constant yield stress versus constant yield stress gradient) the ratio of convective stress over yield stress increases as S^2. Accounting for the increase in density with planet size thus makes plate tectonics more likely with increasing planet size, consistent with the findings of Valencia et al. (2007) and Valencia and O'Connell (2009).

4. Numerical results

4.1. Numerical model and rheology

To perform the numerical experiments we use the latest version of the code StagYY (Tackley, 2008), solving the equations for momentum, energy and conservation of mass in the Bousinesq approximation. For the effect of temperature on viscosity we used an Arrhenius law, choosing activation energy such that there are nine orders of magnitude variation in viscosity from non-dimensional temperatures in the range 0 to 1. The reference viscosity was chosen to be the viscosity at a non-dimensional temperature of 1. The yield stress is implemented through the second invariant of the strain rate tensor. The yield stress is either kept constant or increases linearly with depth.

$$\eta(T) = \exp^{\left[\frac{41.45}{T+1} - \frac{41.45}{2}\right]}. \tag{44}$$

$$\sigma_{yield}(z) = (1-z)\frac{d\sigma_{y-brittle}}{dz}, \tag{45}$$

where $\sigma_{yield}(z)$ is the depth dependent yield stress and $\frac{d\sigma_{y-brittle}}{dz}$ the gradient of the brittle yield stress with depth. These yielding criteria lead to a "yield viscosity", η_{yield}:

$$\eta_{yield} = \frac{\sigma_{yield}(z)}{2\dot{\epsilon}}, \tag{46}$$

where $\dot{\epsilon}$ is the second invariant of the strain rate tensor:

$$\dot{\epsilon} = \sqrt{\frac{1}{2}\dot{\epsilon}_{ij}\dot{\epsilon}_{ij}}. \quad (47)$$

The effective viscosity is defined as:

$$\eta_{eff} = \frac{1}{\frac{1}{\eta(T)} + \frac{1}{\eta_{yield}}}, \quad (48)$$

The constant yield stress was only applied to the top 10% of the domain, a region thick enough to cover the thermal boundary layer. This prevents yielding (i.e. stress dependent reduction of viscosity) in the lower mantle and constrains its effect to the top part of the domain, where it is used to mimic plastic behavior in the lithosphere. The calculations performed by Moresi and Solomatov (1998) did not use a truncated yield stress which resulted in yielding in the deep mantle (L. Moresi, personal communication). Calculations were performed using a 2D Cartesian geometry of aspect ratio 8, using a 64×512 grid with grid refinement at the top and bottom boundaries. Wrap around boundary conditions were applied at the sides. Boundary conditions at the top and bottom were set to be free slip. The temperature at the top boundary was kept at 0. The temperature boundary condition at the bottom was either set to be isothermal at a value of 1 (in the case of basally heated convection), or the heat flux across the lower boundary was set to 0 (in case of internally heated convection).

Four sets of numerical experiments are performed, combining a constant yield stress or a constant yield stress gradient with either basal heating or internal heating mode. For each of these four sets the yield stress (or yield stress gradient) was varied over a range wide enough to observe both mobile and stagnant lid convection. For each set five different sizes of planet were used: $S=1$, $S=1.25$, $S=1.5$, $S=1.75$ and $S=2$. The Rayleigh number was scaled according to Eq. (7), setting $Ra=5\ 10^7$ for a planet of size 1. For the internally heated cases the nondimensional internal heating rate was scaled according to Eq. (8), setting $H=10$ for a planet of size 1. The values for Ra and H for all planet sizes are listed in table 4.1

All calculations were started from the results of an earlier calculation which reached a statistically-steady state mobile lid regime state for the appropriate planet's size and heating mode. Each calculation was then run for a time period corresponding to at least a few billion years, long enough to develop a new statistical-steady state.

4.2. Temperature fields

Snapshots of the temperature and velocity field of representative cases are shown in Fig. 1. With increasing planet size the main visible difference is in the thickness of the boundary layer, otherwise the mobile lid cases look very similar. With increasing friction coefficient (lithospheric strength) the convective regime changes from mobile lid to stagnant lid. For internally-heated convection combined with a constant yield stress gradient an episodic regime was observed at transitional values of yield stress gradient. In some cases with a depth-dependent yield stress an intermediate regime is observed in which a spreading center is present but no focused subduction zone formed, a regime that was also observed by Tackley (2000a) and Solomatov (2004). This regime is indicated separately throughout the figures but is considered mobile lid, since yielding (stress dependent viscosity reduction) is happening, which is what the analytical scalings predict, and because the lid is moving.

4.3. Nondimensional numerical scalings

Fig. 2 shows an overview of the results of all numerical calculations. Nondimensional yield stress or yield stress gradient is plotted versus planet size for each of the four end-member scenarios investigated. We find good agreement between the results of the calculations and the analytical predictions. The numerical results are be used to determine the constant factors in the scaling relationships, which are indicated on Fig. 1. From these graphs it superficially appears that larger planet size strongly favors mobile lid, but this is misleading due to the scaling of dimensional yield stress with planet size discussed in the next section.

4.4. Dimensional numerical scalings

In order to get meaningful results, it is necessary to convert the non-dimensional yield stresses to dimensional values, and the nondimensional yield stress gradients to friction coefficients. To dimensionalise yield stresses we use Eq. (9). The non-dimensional yield stress gradient is dimensionalised via Eq. (11). The dimensional yield stress gradient is then divided by ρg to arrive at the friction coefficient (Eq. (10)). The assumed values for D, κ, η_0, g and ρ listed in Table 2.

Fig. 3 shows an overview of the results of all calculations in dimensional space for the four different end-member scenarios. The analytical predictions given by Eqs. (13), (16), (22) and (24) are also shown, multiplied by a constant factor to fit the numerical results. These graphs show that the numerical results are in agreement with analytical scalings, i.e., that the existence of plate tectonics is roughly independent of planet size, except in the case of basal heating and constant yield stress.

4.5. Intermediate scalings

To verify the assumptions made in deriving the analytical scalings for yield stresses and convective stresses as a function of planet size S we here show some intermediate results. These show that surface velocities v, and lithospheric thickness δ (via Nu) scale with planet size S, i.e. Rayleigh number (Ra or Ra_i) as expected and predicted by boundary layer theory and our analytical scalings.

Fig. 4 shows the relationship between surface velocities and Rayleigh number (Ra for basally heated convection and Ra_i for internally-heated convection). Fig. 4 shows the relationship between Nusselt number and Rayleigh number for the two basally heated scenarios. The cases show a relationship of $Nu \propto Ra^{0.33}$, in agreement with the boundary layer theory (14) used to derive analytical scalings.

5. Discussion

While the obtained scaling relationships seem reliable and robust, care should be taken in interpreting absolute values of (dimensional) critical yield stresses and friction coefficients, because these values depend heavily on our choice of parameter values listed in Table 2, and in any case it is a well-established problem that the values required for mobile lid behavior are lower than what is expected from laboratory rock deformation experiments.

Table 2
Parameters for dimensional scaling.

Quantity	Value at $S=1$	Dependence on S
η_0	10^{21} Pa s	0
κ	10^{-6} m^2/s	0
D	2.89×10^6 m	S
g	10 m/s^2	S
ρ	3300 kg/m^3	0

Our results agree in essence with the scaling studies of Valencia et al. (2007) and Valencia and O'Connell (2009). Although the parameterized models used in this earlier study included more complexities ('realism'), both predict plate tectonics to become more likely with increasing planet size, especially when the effect of increasing density with planet size is taken into account. Also, the findings of Korenaga (2010a) are in line with our results. Remarkably, we reach opposite conclusions to the study of O'Neill and Lenardic (2007). To the best of our knowledge this is because they did not scale all parameters ($Ra, \tilde{H}, \tilde{\sigma}_y$ and $\frac{d\tilde{\sigma}_y}{d\tilde{z}}$) with planet size S in the manner that we argue here is necessary.

The aim of the present study is to explain the basic physics of mantle convection and possibly plate tectonics on super-Earths. The model presented is a highly simplified but general model which can be used as a starting point to investigate the more complex problem of convection and possible plate tectonics on super-Earths. One extension of the model would be to take the pressure and temperature dependence of material properties (including phase changes) of fully compressible convection into account. The appropriate values however are only poorly constrained plus analytical predictions for fully compressible convection will be more difficult to establish. Since pressure in the lower mantle of super-Earths will be up to ten times higher than it is on Earth, proper treatment of its influence is desirable, and might change the dynamics of a planet significantly.

While density increases with pressure, which increases the convective vigor by increasing the acceleration due to gravity and total amount of internal heating (Valencia and O'Connell, 2009; Valencia et al., 2007 and Section 3.3), other physical properties such as viscosity, thermal expansivity and thermal conductivity change with pressure in a way that reduces the effective Rayleigh number, and by a much larger factor than density. Viscosity is generally thought to increase with pressure (e.g. Ammann et al., 2009; Yamazaki and Karato, 2001) although at higher pressures it might start to decrease with pressure due to a change in creep mechanism (Karato, 2011). Additionally a decrease of viscosity is expected at the post-perovskite transition (Ammann et al., 2010), which makes a reliable prediction of the dynamics even more difficult to make. Silicate phases stable beyond the pressure and temperature range at the Earth's core-mantle boundary might drastically change, among others, the thermal conductivity in the deep mantle of super Earths (Umemoto et al., 2006).

Further effects of compressible convection are that thermal expansivity decreases (e.g., Anderson et al., 1992; Chopelas and Boehler, 1992; Katsura et al., 2009) and thermal conductivity increases (e.g. Goncharov et al., 2009; Stackhouse et al., 2010) with pressure. The correct treatment of these effects in parameterized convection models is highly uncertain. One end-member approach is to assume that the top boundary layer (the lithosphere) operates in isolation of the deep mantle and is treated using a local analysis, which assumes that changes in physical properties at higher pressure/depth do not have a significant influence (except for the increase of acceleration due to gravity and the increased internal heating due to higher density), an approach that was used by Valencia et al. (2007) and Valencia and O'Connell (2009). Another end-member approach is to use suitably volume-averaged values of all physical properties in a global boundary layer scaling treatment, in which case the large changes in thermal expansivity and conductivity with pressure would greatly reduce the effective Rayleigh number, as could the presently somewhat uncertain changes in viscosity (Karato, 2011). So, while the former approach predicts greater convective vigor and likelihood of plate tectonics, the latter approach might well do the opposite. In the future, this problem must be resolved by numerical modeling.

To clarify a further simplification, the present calculations assume the Boussinesq approximation, ignoring viscous dissipation and adiabatic heating and cooling in the energy equation, which are known to have some effect on redistributing heat (e.g. Balachandar et al., 1993; Bercovici et al., 1992; Jarvis and McKenzie, 1980). Due to the larger pressure range in a super-Earth's mantle, these effects would be substantially larger than in Earth. We estimate, however, that the dissipation number, which is the nondimensional parameter indicating the magnitude of these effects, is no more than a factor of 2–2.5 larger than in Earth even for the largest (10 Earth mass) planets, so such effects would not be overwhelming.

Other factors one should keep in mind are that the temperature at the core-mantle boundary might be very different from what we used in our model, but to investigate this, one would need information about the thermal history of the super-Earth, including details about its core (for example its relative size, radioactive element concentration etc.). At the present day, one can only speculate about these things.

The way in which we determined whether or not a mobile lid will form crucially depends on the yield stress, or the strength of the lithosphere, which we implicitly assume to be the same on all super-Earths and Earth. In nature, this might not be the case. It is commonly accepted that, among other factors, the presence or absence of liquid water at the planet's surface will affect the strength of the lithosphere. The absence of water might put a super-Earth in the stagnant lid regime, even if our model predicts it to be in the mobile lid regime, similar to the difference between Venus and Earth. There are also some possible effects that originate partly from a nearby star or other planet. These effects can be highly variable and depend on the properties of the other body. Three of these are: 1) The temperature at the planets surface. This might vary widely between planets and will surely have some effect on the formation of a mobile lid on the planet (e.g., Lenardic et al., 2009), since rock strength and the presence of liquid water depend strongly on temperature. Also, the planet's cooling rate and the temperature contrast over the mantle will be affected and thus the style of convection. 2) Tidal forces. Tidal forces might constantly deform the planet and thereby weaken its lithosphere. Also, tidal heating will affect the internal temperature profile and possibly induce melting of rock (as in e.g., Io Tackley et al., 2001). The planet might be tidally locked which could create steep gradients in the temperature at its surface. 3) Giant impacts.

6. Conclusions

Here we have solved the fundamental physics of convection on super-Earths for simplified, end-member cases of basally-heated and internally-heated convection with strongly temperature-dependent viscosity and using either a constant yield stress or a constant yield stress gradient. Analytical scalings and numerical calculations agree. For basally heated convection, plate tectonics is more likely on super-Earths then it is on an Earth-sized planet, becoming increasingly likely with increasing planet size (if a significant amount of basal heating is present). For internally heated convection, plate tectonics is equally likely on super-Earths as on an Earth-sized planet. Our results show that, for this highly simplified system, the effect of planet size on the likelihood of plate tectonics is small and is non-zero only for basally heated convection with constant yield stress. Therefore, it is likely that other factors, such as the presence of liquid water on the surface, have a more important influence on plate tectonics than planet size. For an Earth-like surface environment, based on these first order predictions, we predict super-Earths to have active plate tectonics. Analytical scalings show that this conclusion is strengthened when the effect of increasing density with planet size is taken into consideration. Pressure-variation of other physical parameters viscosity, thermal expansivity and conductivity, is however much higher and might have an opposite effect, which needs to be determined in future numerical studies.

Acknowledgments

This research was supported by SNF grant numbers 200021–112137 and 200020–126773.

References

Ammann, M., Brodholt, J., Dobson, D., 2009. DFT study of migration enthalpies in MgSiO3 perovskite. Phys. Chem. Miner. 36, 151–158. doi:10.1007/s00269-008-0265-z.

Ammann, M., Brodholt, J., Wookey, J., Dobson, D., 2010. First-principles constraints on diffusion in lower-mantle minerals and a weak D" layer. Nature 465, 462–465.

Anderson, D.L., Oda, H., Isaak, D., 1992. A model for the computation of thermal expansivity at high compression and high temperatures — MgO as an example. Geophys. Res. Lett. 19, 1987–1990.

Balachandar, S., Yuen, D.A., Reuteler, D., 1993. Viscous and adiabatic heating effects in 3-Dimensional compressible convection at infinite Prandtl number. Phys. Fluids Fluid Dyn. 5, 2938–2945.

Bercovici, D., 2003. The generation of plate tectonics from mantle convection. Earth Planet. Sci. Lett. 205, 107–121.

Bercovici, D., Schubert, G., Glatzmaier, G., 1992. 3-Dimensional convection of an infinite-Prandtl-number compressible fluid in a basally heated spherical-shell. J. Fluid Mech. 239, 683–719.

Chopelas, A., Boehler, R., 1992. Thermal expansivity in the lower mantle. Geophys. Res. Lett. 19, 1983–1986.

Foley, B., Becker, T.W., 2009. Generation of plate tectonics and mantle heterogeneity from a spherical, visco-plastic convection model. Geochem. Geophys. Geosyst. 10.

Fowler, A., O'Brien, B., 2003. Lithospheric failure on Venus. Proc. R. Soc. Lond. 459, 2663–2704.

Goncharov, A.F., Beck, P., Struzhkin, V.V., Haugen, B., Jacobsen, S.D., 2009. Thermal conductivity of lower-mantle minerals. Phys. Earth Planet. Inter. 174, 24–32.

Ida, S., Lin, D., 2004. Toward a deterministic model of planetary formation. I. A desert in the mass and semimajor axis distributions of extrasolar planets. ApJ 604, 388–413.

Jarvis, G.T., McKenzie, D.P., 1980. Convection in a compressible fluid with infinite Prandtl number. J. Fluid Mech. 96, 515–583.

Karato, S.-i., 2011. Rheological structure of the mantle of a super-Earth: some insights from mineral physics. Icarus 212 (1), 14–23. ISSN 0019-1035. doi:10.1016/j.icarus.2010.12.005.

Katsura, I., et al., 2009. P-V-T relations of MgSiO3 perovskite determined by in situ X-ray diffraction using a large-volume high-pressure apparatus. Geophys. Res. Lett. 36.

Kohlstedt, D.L., Evans, B., Mackwell, S.J., 1995. Strength of the lithosphere: constraints imposed by laboratory experiments. J. Geophys. Res. 100, 17587–17602.

Korenaga, J., 2010a. On the likelihood of plate tectonics on super-Earths: does size matter? Astrophys. J. Lett. 725, 43–46.

Korenaga, J., 2010b. Scaling of plate-tectonic convection with pseudoplastic rheology. JRL 115.

Lenardic, A., Jellinek, A.M., Moresi, L.N., 2009. A climate induced transition in the tectonic style of a terrestrial planet. Earth Planet. Sci. Lett. 271, 34–42.

Loddoch, A., Stein, C., Hansen, U., 2006. Temporal variations in the convective style of planetary mantles. Earth Planet. Sci. Lett. 251, 79–89.

Moresi, L.N., Solomatov, V.S., 1995. Numerical investigations of 2D convection with extremely large viscosity variations. Phys. Fluids 7, 2154–2162.

Moresi, L.N., Solomatov, V., 1998. Mantle convection with a brittle lithosphere: thoughts on the global tectonic styles of the Earth and Venus. Geophys. J. Int. 133, 669–682.

Muhlhaus, H.B., Regenauer-Lieb, K., 2005. Towards a self-consistent plate mantle model that includes elasticity: simple benchmarks and application to basic modes of convection. Geophys. J. Int. 163, 788–800.

O'Neill, C., Lenardic, A., 2007. Geological consequences of super-sized Earths. Geophys. Res. Lett. 34.

Ogawa, M., 2003. Plate-like regime of a numerically modeled thermal convection in a fluid with temperature-, pressure-, and stress-history-dependent viscosity. JGR 2067–2072.

Richards, M., Yang, W.S., Baumgardner, J., Bunge, H.P., 2001. Role of a low-viscosity zone in stabilizing plate tectonics: implications for comparative terrestrial planetology. Geochem. Geophys. Geosyst. 2.

Solomatov, V.S., 1995. Scaling of temperature- and stress-dependent viscosity convection. Phys. Fluids 7, 266–274.

Solomatov, V.S., 2004. Initiation of subduction by small-scale convection. J. Geophys. Res. 109.

Stackhouse, S., Stixrude, L., Karki, B.B., 2010. Thermal conductivity of periclase (MgO) from first principles. Phys. Rev. Lett. 104, 208501.

Stein, C., Schmalzl, J., Hansen, U., 2004. The effect of rheological parameters on plate behaviour in a self-consistent model of mantle convection. Phys. Earth Planet. Inter. 142, 225–255.

Tackley, P.J., 2000a. Self-consistent generation of tectonic plates in time-dependent, three-dimensional mantle convection simulations 1. Pseudoplastic yielding. Geochem. Geophys. Geosyst. 1.

Tackley, P.J., 2000b. Self-consistent generation of tectonic plates in time-dependent, three-dimensional mantle convection simulations 2. Strain weakening and asthenosphere. Geochem. Geophys. Geosyst. 1.

Tackley, P.J., 2008. Modelling compressible mantle convection with large viscosity contrasts in a three-dimensional spherical shell using the yin-yang grid. Phys. Earth Planet. Inter. 171, 7–18.Recent Advances in Computational Geodynamics: Theory, Numerics and Applications

Tackley, P.J., van Heck, H.J., 2008. Mantle convection, stagnant lids and plate tectonics on super-Earths. EOS Trans. AGU 89 (Fall Meet. Suppl., Abstract P14B–03).

Tackley, P.J., Schubert, G., Glatzmaier, G.A., Schenk, P., Ratcliff, J.T., Matas, J.P., 2001. Three-dimensional simulations of mantle convection in Io. Icarus (USA) 149 (1), 79–93.

Trompert, R., Hansen, U., 1998. Mantle convection simulations with rheologies that generate plate-like behaviour. Nature 395, 686–689.

Turcotte, D.L., Schubert, G., 1982. Applications of continuum physics to geological problems. Geodynamics. John Wiley, New York.

Umemoto, K., Wentzcovitch, R.M., Allen, P.B., 2006. Dissociation of MgSiO3 in the cores of gas giants and terrestrial exoplanets. Science 311, 983–986.

Valencia, D., O'Connell, R.J., 2009. Convection scaling and subduction on Earth and super-Earths. Earth Planet. Sci. Lett. 286, 492–502.

Valencia, D., O'Connell, R.J., Sasselov, D.D., 2007. Inevitability of plate tectonics on super-Earths. ApJ 670.

van Heck, H.J., Tackley, P.J., 2008. Planforms of self-consistently generated plates in 3-d spherical geometry. Geophys. Res. Lett. 35.

Yamazaki, D., Karato, S., 2001. Some mineral physics contraints on the rheology and geothermal structure of earth's lower mantle. Am. Mineralog. 86, 385–391.

Yoshida, M., 2008. Mantle convection with longest-wavelength thermal heterogeneity in a 3-d spherical model: degree one or two? GRL 35.

Yoshida, M., 2010. Temporal evolution of the stress state in a supercontinent during mantle reorganization. GJI 180.